

Dynamic stability of a metal foam rectangular plate

D. Debowski^{1*}, K. Magnucki^{2,3} and M. Malinowski¹

¹*Institute of Mechanical Engineering and Machine Operation, University of Zielona Gora, ul. Podgorna 50, PL. 65-246 Zielona Gora, Poland*

²*Institute of Applied Mechanics, Poznan University of Technology, ul. Piotrowo 3, PL. 60-965 Poznan, Poland*

³*Institute of Rail Vehicles "TABOR", ul. Warszawska 181, PL. 61-055 Poznan, Poland*

(Received July 15, 2009, Accepted February 24, 2010)

Abstract. The subject of the paper is an isotropic metal foam rectangular plate. Mechanical properties of metal foam vary continuously through plate of the thickness. A nonlinear hypothesis of deformation of plane cross section is formulated. The system of partial differential equations of the plate motion is derived on the basis of the Hamilton's principle. The system of equations is analytically solved by the Bubnov-Galerkin method. Numerical investigations of dynamic stability for family rectangular plates with respect analytical solution are performed. Moreover, FEM analysis and theirs comparison with results of numerical-analytical calculations are presented in figures.

Keywords: metal foam plate; dynamic stability; elastic buckling; shear effect.

1. Introduction

Instability phenomenon of constructions is one of the most important problems contemporary industry. Plates as elementary parts of a construction are particularly subject on this kind problems. The present technology allows to improve mechanical properties, and the same resistances on buckling through the change of the construction or the use of new materials. In this paper submit the rectangular plate made of porous-cellular alloys.

Porous materials belong to structures, in which mechanical properties are usually constant or variable through thickness. The first general and universal review of mechanical and thermal properties these materials were presented by Evans *et al.* (1999). Ashby *et al.* (2000) presented the novel mechanical, physical, thermal and acoustical properties of metal foams, their performance, their manufacture and their utilization in weight-dependent applications in various industries. Banhart (2001) were described experimental investigations, manufacturing process and the application of the porous materials. More over, physical constants of porous-cellular metals are analytically and experimentally estimated. Bart-Smith *et al.* (2001) have been measured and simulated the bending performance of sandwich beam with porous cores. Correlation between Young's and shear modulus and porosity in porous material presented by Kovacic (1999, 2001). Choi and Lakes (1995) modeled and carried out experiments of Young's moduli and mass density of conventional and re-entrant open cells foams. It the ability of absorption through

*Corresponding author, Ph.D., E-mail: D.Debowski@ibem.uz.zgora.pl

porous materials energy was presented by Ramamurty and Paul(2004).

The classical theory of rectangular plates according to Kirchhoff-Love's hypothesis for non-homogeneous materials usually the linear dependence between in-plane displacements and deflection are assumed. Advantages of this approach are simplicity and ability to the use of solutions that is derived for homogeneous plates. The main disadvantage is neglecting shear forces and displacements, which restrict using this approach to thin plates without rapid changes of mechanical properties. In order to overcome the aforementioned difficulties a lot of higher order hypotheses, which include shearing is applied for example by Wang *et al.* (2000), Yang *et al.* (2006), Bakker *et al.* (2007) . A thorough review of theories, including zig-zag ones, used for modeling of multilayered plates and comprehensively bibliography may be found in the works of Carrera (2000, 2001, 2003). A refined nonlinear zig-zag first-order shear deformation theory of composite laminated plates using a modified version of Reissner's mixed variational formulation was presented by Fares and Elmaghany (2008).

Carrera *et al.* (2008) formulated the kinematic model for analysis of functionally graded material plate subjected to transverse loadings. Reddy (2000) obtained the Navier's solution of rectangular and trough-thickness functionally graded plates using finite element models and incorporating third-order shear deformation theory and von Karman-type geometric non-linearity. Results devoted to bending and buckling (in a static sense) of porous beams may be found in works of Magnucki and Stasiewicz (2004a, b). A discussion on porous rectangular plates carried out Magnucki *et al.* (2006), and porous cylindrical panel Malinowski and Magnucki (2005) respectively. The results of numerical analysis of such construction of a wagon roof of railway vehicles Mielniczuk *et al.* (2006), have been obtained.

A model of porous material with variable porosity through out the thickness of the plate applied in the thin-walled construction are presented e.g., in the work of Mielniczuk and Malinowski (2005). In that model, it is assumed that modulus of elasticity is varied across the thickness and depends on the material porosity. The analytical studies of strength and stability of porous constructions allowed for non-linear hypothesis of the deformation into account have been taken are presented in many papers.

The dynamic stability of plates is a subject of many papers in recent years. The latest research in the field of vibration of composite shell and plates presented Qatu (2004). Sahu and Datta (2007) presented the review of works carried out the dynamic stability of plates and shells in years 1987-2005. Szcześniak (2000) described of forced vibration of the plate with assumed a non-linear hypothesis. This author assumed that forced vibration is dependent on load impulse, and the other loads. Nonlinear dynamic buckling of stiffened plate under in-plane impact load was described in the paper of Zhang *et al.* (2004). Eshmatov (2007) used the Kirchhoff-Love hypothesis and Reissner-Mindlin generalized theory in geometrically nonlinear statements. This autor described the analyses of the nonlinear vibrations and dynamic stability of viscoelastic orthotropic plates. Mathematical model of the dynamic stability of the porous-cellular rectangular plate under pulsating compression load is presented in the work of Debowski and Magnucki (2006). Experimental studies with axially impacted laminated composite plates may be found in the work of Abramowich and Grunwald(1995).

In this paper the dynamic stability of a metal foam rectangular plate is presented.

2. Mathematical model of the rectangular plate

The subject of the paper is an isotropic metal foam rectangular plate with four simply supported edges. The dimensions of the plate are length a , width b and thickness t . The plate is oriented in the coordinate system x,y,z , but the plane xy it's middle plane of the plate. The plate is subjected to uniform

compressive forces $N_x(\tau)$, $N_y(\tau)$ which is directly proportional to the time τ (Fig. 1).

A porous plate is a generalized sandwich plate. Its outside surfaces (top and bottom) are smooth, without pores, whereas inside the plate is porous. The coefficient of the plate porosity e_0 varies in the normal direction to middle surface of the plate and assuming the minimal value in the middle surface of the plate. The mechanical properties of the plate vary across its thickness t and depend on porosity of plate (Fig. 2). The minimal value of Young's modulus E_0 occurs in the middle surface of the plate and maximal values E_1 occur at its top and bottom surfaces.

Moduli of elasticity of the metal foam plate are defined as described by Magnucki and Stasiewicz (2004a, b) and have following form

$$E(z) = E_1[1 - e_0 \cos(\pi\zeta)], \quad G(z) = G_1[1 - e_0 \cos(\pi\zeta)] \quad (1)$$

where:

$$e_0 = 1 - \frac{E_0}{E_1} = 1 - \frac{G_0}{G_1} - \text{dimensionless coefficient of the porosity } 0 \leq e_0 \leq 1$$

E_0, G_0, E_1, G_1 – moduli of elasticity for $\zeta = 0$ and $\zeta = \pm 1/2$, respectively

$$G_j = \frac{E_j}{2(1 + \nu)} - \text{relationship between the moduli of elasticity for } j = 0, 1$$

$$\zeta = \frac{z}{t} - \text{dimensionless coordinate}$$

ν – Poisson's ratio

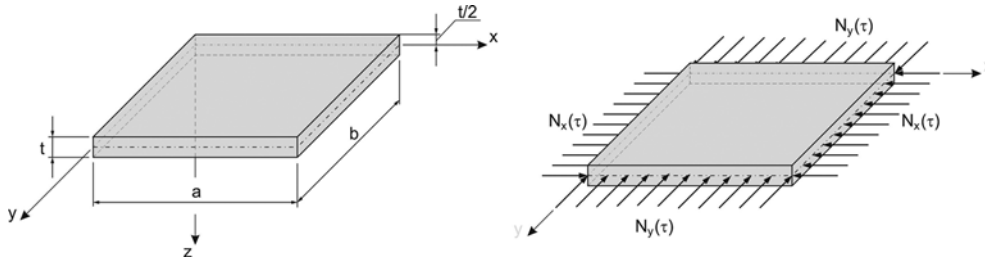


Fig. 1 Metal foam rectangular plate

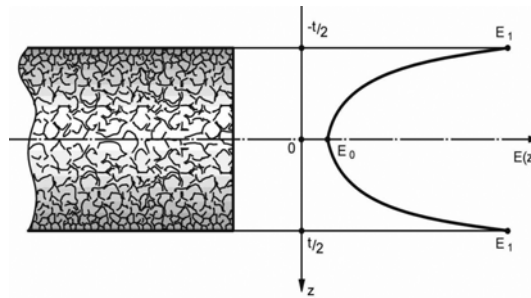


Fig. 2 Structure scheme of a plate

The material is of continuous mechanical properties. Relations between Young's modulus and mass density of foam metallic materials were presented by Choi and Lakes (1995). If we take into consideration these results, mass density is expressed as below

$$\rho(\zeta) = \rho_1 [1 - e_m \cos(\pi\zeta)] \quad (2)$$

where:

ρ_0, ρ_1 – mass densities of the metal for $\zeta = 0$ and $\zeta = 1/2$, respectively

$e_m = 1 - \sqrt{1 - e_0}$ – dimensionless parameter of the mass density

The nonlinear hypothesis of deformation of a plane cross section of the plate is assumed (Fig.3). A flat plane of a cross-section is perpendicular to the mid-plane of a plate before deformation and changes after deformation to a surface, which is only perpendicular to the outer planes of the plate ($z = \pm t/2$).

A displacement field of any cross-section of a plate was defined by the following form

$$u(x, y, z, \tau) = u_0(x, y, \tau) + \left\{ -t \left\{ \zeta \frac{\partial w}{\partial x} - \frac{1}{\pi} [\psi_1(x, y, \tau) \sin(\pi\zeta) + \psi_2(x, y, \tau) \sin(2\pi\zeta) \cos^2(\pi\zeta)] \right\} \right\} \quad (3)$$

$$v(x, y, z, \tau) = v_0(x, y, \tau) + \left\{ -t \left\{ \zeta \frac{\partial w}{\partial y} - \frac{1}{\pi} [\phi_1(x, y, \tau) \sin(\pi\zeta) + \phi_2(x, y, \tau) \sin(2\pi\zeta) \cos^2(\pi\zeta)] \right\} \right\} \quad (4)$$

$$w(x, y, z, \tau) = w(x, y, 0, \tau) = w(x, y, \tau) \quad (5)$$

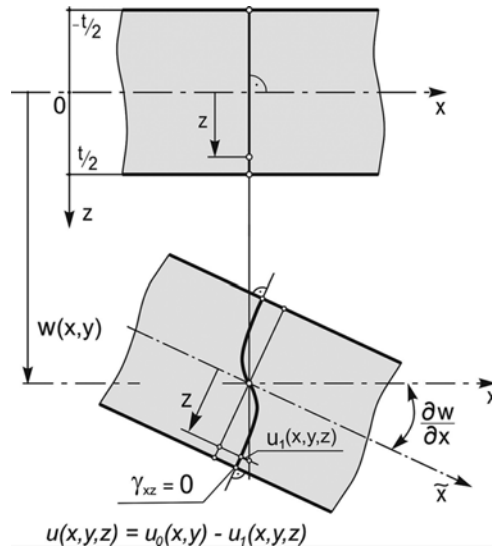


Fig. 3 Scheme of deformation of a plane cross section of a plate

Here exist three autonomous functions, where: τ – time, $w(x,y,\tau)$ – lateral displacement (deflection of the plate), $\psi(x,y,\tau)$ and $\phi(x,y,\tau)$ – dimensionless functions of displacement, $u_0(x,y,\tau)$, $v_0(x,y,\tau)$ displacements in the plane of the plate in the x , y direction respectively.

Strains state of the plate describing the geometric relationships for the plate are defined as follows

$$\varepsilon_x = \frac{\partial u}{\partial x} + \frac{1}{2} \left(\frac{\partial w}{\partial x} \right)^2 = \frac{\partial u_0}{\partial x} - t \left\{ \zeta \frac{\partial^2 w}{\partial x^2} - \frac{1}{\pi} \left[\frac{\partial \psi}{\partial x} \sin(\pi \zeta) + \frac{\partial \psi_2}{\partial x} \sin(2\pi \zeta) \cos^2(\pi \zeta) \right] \right\} + \frac{1}{2} \left(\frac{\partial w}{\partial x} \right)^2 \quad (6)$$

$$\varepsilon_y = \frac{\partial v}{\partial y} + \frac{1}{2} \left(\frac{\partial w}{\partial y} \right)^2 = \frac{\partial v_0}{\partial y} - t \left\{ \zeta \frac{\partial^2 w}{\partial y^2} - \frac{1}{\pi} \left[\frac{\partial \phi_1}{\partial x} \sin(\pi \zeta) + \frac{\partial \phi_2}{\partial x} \sin(2\pi \zeta) \cos^2(\pi \zeta) \right] \right\} + \frac{1}{2} \left(\frac{\partial w}{\partial y} \right)^2 \quad (7)$$

$$\gamma_{xy} = \frac{\partial u}{\partial y} + \frac{\partial v}{\partial x} + \frac{\partial w}{\partial x} \cdot \frac{\partial w}{\partial y} = \frac{\partial u_0}{\partial x} + \frac{\partial v_0}{\partial y} +$$

$$-t \left\{ 2\zeta \frac{\partial^2 w}{\partial x \partial y} - \frac{1}{\pi} \left[\left(\frac{\partial \psi_1}{\partial y} + \frac{\partial \phi_1}{\partial x} \right) \sin(\pi \zeta) + \left(\frac{\partial \psi_2}{\partial y} + \frac{\partial \phi_2}{\partial x} \right) \sin(2\pi \zeta) \cos^2(\pi \zeta) \right] \right\} + \frac{\partial w}{\partial x} \cdot \frac{\partial w}{\partial y} \quad (8)$$

$$\gamma_{xz} = \frac{\partial u}{\partial z} + \frac{\partial w}{\partial x} = \psi_1(x,y) \cos(\pi \zeta) + \psi_2(x,y) [\cos(2\pi \zeta) + \cos(4\pi \zeta)] \quad (9)$$

$$\gamma_{yz} = \frac{\partial v}{\partial z} + \frac{\partial w}{\partial y} = \phi_1(x,y) \cos(\pi \zeta) + \phi_2(x,y) [\cos(2\pi \zeta) + \cos(4\pi \zeta)] \quad (10)$$

The physical relationships, according to Hooke's law, are

$$\sigma_x = \frac{E(\zeta)}{1-\nu^2} (\varepsilon_x + \nu \varepsilon_y), \quad \sigma_y = \frac{E(\zeta)}{1-\nu^2} (\varepsilon_y + \nu \varepsilon_x)$$

$$\tau_{xy} = G(z) \cdot \gamma_{xy}, \quad \tau_{xz} = G(z) \cdot \gamma_{xz}, \quad \tau_{yz} = G(z) \cdot \gamma_{yz} \quad (11)$$

3. System of partial differential equations of metal foam plate

The equation of the motion of a rectangular plate can be obtained by the Hamilton's principle

$$\delta \int_{\tau_0}^{\tau_1} [T_K - (U_\varepsilon - W)] d\tau = 0 \quad (12)$$

where:

U_ε is the elastic strain energy

$$U_\varepsilon = \frac{t}{2} \int_{\Omega} \int_{-1/2}^{1/2} (\sigma_x \varepsilon_x + \sigma_y \varepsilon_y + \tau_{xy} \gamma_{xy} + \tau_{xz} \gamma_{xz} + \tau_{yz} \gamma_{yz}) dx dy d\zeta \quad (13)$$

T_K is the kinetic energy

$$T_K = \frac{t}{2} \int_{-1/2}^{1/2} \int_0^a \int_0^b \rho(\zeta) \left(\frac{\partial w}{\partial \tau} \right)^2 dx dy d\zeta \quad (14)$$

The work W of the external loads is defined with allowance for boundary conditions and will be presented in the following part of the work.

Basing on the Hamilton's principle Eq. (12), and after the integrating on the interval $-1/2 \leq \zeta \leq 1/2$ and the integrating by parts over the mid-plane of the plate a system of seven partial differential equations and system of boundary conditions were obtained

$$\begin{aligned} \delta w) \quad & \frac{E_1 t}{(1-\nu^2)} \left\{ \left[c_1 t^2 \nabla w - c_2 t^2 \left(\frac{\partial}{\partial x} (\nabla^2 \psi_1) + \frac{\partial}{\partial y} (\nabla^2 \phi_1) \right) - c_3 t^2 \left(\frac{\partial}{\partial x} (\nabla^2 \psi_2) \right. \right. \right. \\ & \left. \left. \left. + \frac{\partial}{\partial y} (\nabla^2 \phi_2) \right) \right] + c_{24} \left[\left(\frac{\partial w}{\partial x} \right)^2 \left[-\frac{3}{2} \frac{\partial^2 w}{\partial x^2} - \frac{1}{2} \frac{\partial^2 w}{\partial y^2} \right] + \left(\frac{\partial w}{\partial y} \right)^2 \left[-\frac{3}{2} \frac{\partial^2 w}{\partial y^2} - \frac{1}{2} \frac{\partial^2 w}{\partial x^2} \right] + \right. \\ & - 2 \frac{\partial w}{\partial x} \frac{\partial^2 w}{\partial x \partial y} \frac{\partial w}{\partial y} - \frac{\partial w}{\partial x} \left[\frac{\partial^2 u_0}{\partial x^2} + \frac{(1-\nu)}{2} \frac{\partial^2 u_0}{\partial y^2} + \frac{(1+\nu)}{2} \frac{\partial^2 v_0}{\partial x \partial y} \right] - \frac{\partial w}{\partial y} \left[\frac{\partial^2 v_0}{\partial y^2} + \frac{(1-\nu)}{2} \right. \\ & \left. \left. \left. \cdot \frac{\partial^2 v_0}{\partial x^2} + \frac{(1+\nu)}{2} \frac{\partial^2 u_0}{\partial x \partial y} \right] - \frac{\partial u_0}{\partial x} \left[\frac{\partial^2 w}{\partial x^2} + \nu \frac{\partial^2 w}{\partial y^2} \right] - \frac{\partial v_0}{\partial y} \left[\frac{\partial^2 w}{\partial y^2} + \nu \frac{\partial^2 w}{\partial x^2} \right] - (1-\nu) \frac{\partial^2 w}{\partial x \partial y} \right. \\ & \left. \left. \left. \cdot \left[\frac{\partial u_0}{\partial y} + \frac{\partial v_0}{\partial x} \right] \right] \right\} + t \rho_1 c_{11} \frac{\partial^2 w}{\partial \tau^2} = 0 \end{aligned} \quad (15)$$

$$\delta u_0) \quad \frac{\partial^2 u_0}{\partial x^2} + \frac{\partial w}{\partial x} \frac{\partial^2 w}{\partial x^2} + \frac{1+\nu}{2} \frac{\partial^2 v_0}{\partial x \partial y} + \frac{1+\nu}{2} \frac{\partial w}{\partial y} \frac{\partial^2 w}{\partial x \partial y} + \frac{1-\nu}{2} \frac{\partial^2 u_0}{\partial y^2} + \frac{1-\nu}{2} \frac{\partial w}{\partial x} \frac{\partial^2 w}{\partial y^2} = 0 \quad (16)$$

$$\delta v_0) \quad \frac{\partial^2 v_0}{\partial y^2} + \frac{\partial w}{\partial y} \frac{\partial^2 w}{\partial y^2} + \frac{1+\nu}{2} \frac{\partial^2 u_0}{\partial x \partial y} + \frac{1+\nu}{2} \frac{\partial w}{\partial x} \frac{\partial^2 w}{\partial x \partial y} + \frac{1-\nu}{2} \frac{\partial^2 v_0}{\partial x^2} + \frac{1-\nu}{2} \frac{\partial w}{\partial y} \frac{\partial^2 w}{\partial x^2} = 0 \quad (17)$$

$$\begin{aligned} \delta \psi_1) \quad & c_2 \frac{\partial}{\partial x} (\nabla^2 w) - c_4 \left[\frac{\partial^2 \psi_1}{\partial x^2} + \frac{1-\nu}{2} \frac{\partial^2 \psi_1}{\partial y^2} + \frac{1+\nu}{2} \frac{\partial^2 \phi_1}{\partial x \partial y} \right] - c_5 \left[\frac{\partial^2 \psi_2}{\partial x^2} + \frac{1-\nu}{2} \frac{\partial^2 \psi_2}{\partial y^2} \right. \\ & \left. + \frac{1+\nu}{2} \frac{\partial^2 \phi_2}{\partial x \partial y} \right] + \frac{1-\nu}{2 t^2} [c_7 \psi_1 + c_8 \psi_2] = 0 \end{aligned} \quad (18)$$

$$\begin{aligned}
\delta\phi_1) \quad & c_2 \frac{\partial}{\partial y} (\nabla^2 w) - c_4 \left[\frac{\partial^2 \phi_1}{\partial y^2} + \frac{1-\nu}{2} \frac{\partial^2 \phi_1}{\partial x^2} + \frac{1+\nu}{2} \frac{\partial^2 \psi_1}{\partial x \partial y} \right] - c_5 \left[\frac{\partial^2 \phi_2}{\partial y^2} + \frac{1-\nu}{2} \frac{\partial^2 \phi_2}{\partial x^2} \right. \\
& \left. + \frac{1+\nu}{2} \frac{\partial^2 \psi_2}{\partial x \partial y} \right] + \frac{1-\nu}{2t^2} [c_7 \phi_1 + c_8 \phi_2] = 0
\end{aligned} \tag{19}$$

$$\begin{aligned}
\delta\psi_2) \quad & c_3 \frac{\partial}{\partial x} (\nabla^2 w) - c_5 \left[\frac{\partial^2 \psi_1}{\partial x^2} + \frac{1-\nu}{2} \frac{\partial^2 \psi_1}{\partial y^2} + \frac{1+\nu}{2} \frac{\partial^2 \phi_1}{\partial x \partial y} \right] - c_6 \left[\frac{\partial^2 \psi_2}{\partial x^2} + \frac{1-\nu}{2} \frac{\partial^2 \psi_2}{\partial y^2} \right. \\
& \left. + \frac{1+\nu}{2} \frac{\partial^2 \phi_2}{\partial x \partial y} \right] + \frac{1-\nu}{2t^2} [c_8 \psi_1 + c_9 \psi_2] = 0
\end{aligned} \tag{20}$$

$$\begin{aligned}
\delta\phi_2) \quad & c_3 \frac{\partial}{\partial y} (\nabla^2 w) - c_5 \left[\frac{\partial^2 \phi_1}{\partial y^2} + \frac{1-\nu}{2} \frac{\partial^2 \phi_1}{\partial x^2} + \frac{1+\nu}{2} \frac{\partial^2 \psi_1}{\partial x \partial y} \right] - c_6 \left[\frac{\partial^2 \phi_2}{\partial y^2} + \frac{1-\nu}{2} \frac{\partial^2 \phi_2}{\partial x^2} \right. \\
& \left. + \frac{1+\nu}{2} \frac{\partial^2 \psi_2}{\partial x \partial y} \right] + \frac{1-\nu}{2t^2} [c_8 \phi_1 + c_9 \phi_2] = 0
\end{aligned} \tag{21}$$

where: $c_1 = \frac{1}{12} \left(1 - \frac{\pi^2 - 8}{2\pi^3} e_0 \right)$, $c_2 = \frac{1}{\pi^2} \left(\frac{2}{\pi} - \frac{1}{4} e_0 \right)$, $c_3 = \frac{1}{\pi^2} \left(\frac{3}{16} - \frac{32}{75\pi} e_0 \right)$, $c_4 = \frac{1}{\pi^2} \left(\frac{1}{2} - \frac{2}{3\pi} e_0 \right)$

$c_5 = \frac{1}{\pi^2} \left(\frac{8}{15\pi} - \frac{1}{8} e_0 \right)$, $c_6 = \frac{1}{\pi^2} \left(\frac{5}{32} - \frac{128}{315\pi} e_0 \right)$, $c_7 = \frac{1}{2} - \frac{4}{3\pi} e_0$, $c_8 = \frac{8}{15\pi} - \frac{1}{4} e_0$, $c_9 = 1 - \frac{832}{315\pi} e_0$

$c_{11} = 1 - \frac{2}{\pi} e_m$, $c_{24} = 1 - \frac{2}{\pi} e_0$

The system of partial differential equations was transformed to the system of four fundamental differential equations. For that purpose stresses and internal forces into plate were calculated. The finite deflection hypothesis of thin plate was assumed.

Components of internal normal and shear components are

$$N_x = \int_{-t/2}^{t/2} \sigma_x dz, \quad N_y = \int_{-t/2}^{t/2} \sigma_y dz, \quad S_{xy} = \int_{-t/2}^{t/2} \tau_{xy} dz \tag{22}$$

$$Q_x = \int_{-t/2}^{t/2} \tau_{xz} dz, \quad Q_y = \int_{-t/2}^{t/2} \tau_{yz} dz \tag{23}$$

and moments

$$M_x = \int_{-t/2}^{t/2} \sigma_x z dz, \quad M_y = \int_{-t/2}^{t/2} \sigma_y z dz, \quad M_{xy} = \int_{-t/2}^{t/2} \tau_{xy} z dz \quad (24)$$

Normal and shear loads can be expressed with the stress function $F(x,y)$, and unknown function $\psi_1, \psi_2, \Phi_1, \Phi_2$ have the form

$$N_x = \frac{\partial^2 F}{\partial y^2}, \quad N_y = \frac{\partial^2 F}{\partial x^2}, \quad S_{xy} = -\frac{\partial^2 F}{\partial x \partial y} \quad (25)$$

$$\psi_1 = \frac{\partial \Phi_1}{\partial x}, \quad \phi_1 = \frac{\partial \Phi_1}{\partial y}, \quad \psi_2 = \frac{\partial \Phi_2}{\partial x}, \quad \phi_2 = \frac{\partial \Phi_2}{\partial y} \quad (26)$$

Eqs. (18), (19), (20), (21) with the help of the displacement functions Φ_1, Φ_2 to the two differential equation were transformed. When we use equation of strains continuity the system of four fundamentals equations of dynamic stability was obtained

$$\frac{E_1 t^3}{(1-\nu^2)} [c_1 \nabla^4 w - c_2 \nabla^4 \Phi_1 - c_3 \nabla^4 \Phi_2] - L(w, F) = -t \rho_1 c_{11} \frac{\partial^2 w}{\partial \tau^2} \quad (27)$$

$$c_2 \nabla^4 w - c_4 \nabla^4 \Phi_1 - c_5 \nabla^4 \Phi_2 + \frac{1-\nu}{2t^2} [c_7 \nabla^2 \Phi_1 + c_8 \nabla^2 \Phi_2] = 0 \quad (28)$$

$$c_3 \nabla^4 w - c_5 \nabla^4 \Phi_1 - c_6 \nabla^4 \Phi_2 + \frac{1-\nu}{2t^2} [c_8 \nabla^2 \Phi_1 + c_9 \nabla^2 \Phi_2] = 0 \quad (29)$$

$$\frac{1}{c_0 E_1 t} \nabla^4 F = -\frac{1}{2} L(w, w) \quad (30)$$

where:

$$\nabla^2 = \frac{\partial^2}{\partial x^2} + \frac{\partial^2}{\partial y^2}, \quad \text{-- Laplace operator, } \nabla^4 = \frac{\partial^4}{\partial x^4} + 2 \frac{\partial^4}{\partial x^2 \partial y^2} + \frac{\partial^4}{\partial y^4}$$

$$L(w, F) = \frac{\partial^2 w}{\partial x^2} \frac{\partial^2 F}{\partial y^2} - 2 \frac{\partial^2 w}{\partial x \partial y} \frac{\partial^2 F}{\partial x \partial y} + \frac{\partial^2 w}{\partial y^2} \frac{\partial^2 F}{\partial x^2} \text{-- non-linear operator}$$

$$L(w, w) = 2 \left(\frac{\partial^2 w}{\partial x^2} \frac{\partial^2 w}{\partial y^2} \right) - 2 \left(\frac{\partial^2 w}{\partial x \partial y} \right)^2$$

Boundary conditions for the simply supported plate are

$$\begin{aligned} 0 \leq y \leq b, \frac{\partial^2 F}{\partial y^2} \Big|_{x=0, a} &= N_x^0, \quad M_x \Big|_{x=0, a} = 0, \quad w \Big|_{x=0, a} = 0 \\ 0 \leq x \leq a, \frac{\partial^2 F}{\partial x^2} \Big|_{x=0, b} &= N_y^0, \quad M_y \Big|_{y=0, b} = 0, \quad w \Big|_{y=0, b} = 0 \end{aligned} \quad (31)$$

4. Solution of dynamic stability problem of metal foam plate

The basic system of differential equations Eqs. (27), (28), (29), (30) was approximately solved with the use of the Bubnov-Galerkin method. The form of unknown functions were assumed as bellow

$$w(x, y, \tau) = f_1(\tau) \cdot \sin \frac{m\pi x}{a} \sin \frac{n\pi y}{b} \quad (32)$$

$$\Phi_1(x, y, \tau) = f_1(\tau) \alpha_{\Phi 1} \sin \frac{m\pi x}{a} \sin \frac{n\pi y}{b} \quad (33)$$

$$\Phi_2(x, y, \tau) = f_1(\tau) \alpha_{\Phi 2} \sin \frac{m\pi x}{a} \sin \frac{n\pi y}{b} \quad (34)$$

where: m, n - natural numbers, $f_1(\tau)$ — displacement dependent on the time.

The exact solution can be constructed when the plate has a rectangular geometry with the simply supported edge conditions. The Eqs. (32), (33), (34) satisfy boundary conditions.

Solving Eqs. (28), (29) following relationships were obtained

$$\alpha_{\Phi 1} = \frac{b_1 a_{22} - b_2 a_{12}}{a_{11} a_{22} - a_{12}^2}, \quad \alpha_{\Phi 2} = \frac{b_2 a_{11} - a_{21} b_1}{a_{11} a_{22} - a_{12}^2} \quad (35)$$

where:

$$\begin{aligned} a_{11} &= c_4 k + c_7 \frac{1-\nu}{2t^2}, \quad a_{12} = c_5 k + c_8 \frac{1-\nu}{2t^2}, \quad a_{22} = c_6 k + c_9 \frac{1-\nu}{2t^2} \\ a_{12} &= a_{21}, \quad b_1 = c_2 k, \quad b_2 = c_3 k, \quad k = \left(\frac{m\pi}{a} \right)^2 \left[1 + \left(\frac{n}{m} \frac{a}{b} \right)^2 \right] \end{aligned}$$

On the grounds of the Eq. (30) and giving consideration to equation of strains continuity the stress function can be expressed as below

$$F(x, y) = c_0 E_1 t \left\{ f_1^2 \left(\alpha_{k1} \cos 2 \frac{n\pi y}{b} + \alpha_{k2} \cos 2 \frac{m\pi x}{a} \right) \right\} + \frac{1}{2} N_x^0 y^2 + \frac{1}{2} N_y^0 x^2 \quad (36)$$

where:

$$\alpha_{k1} = \frac{1}{32} \left(\frac{m}{a} \right)^2 \left(\frac{b}{n} \right)^2, \quad \alpha_{k2} = \frac{1}{32} \left(\frac{n}{b} \right)^2 \left(\frac{a}{m} \right)^2$$

Substitution of the Eqs. (32), (33), (34), (35), (36) into Eq. (27) and using the Bubnov-Galerkin method differential equation of motion can be expressed as

$$\begin{aligned} \frac{\partial^2 \tilde{f}_1}{\partial \tau^2} = & \frac{m^2 \pi^2}{a^2 c_{11} \rho_1} \left\{ -\frac{E_1 t^2}{(1-\nu^2)} \left[(c_1 - c_2 \alpha_{\Phi_1} - c_3 \alpha_{\Phi_2}) \left(\frac{m\pi}{a} \right)^2 \left[1 + \left(\frac{n a}{m b} \right)^2 \right]^2 \right] \tilde{f}_1 \right. \\ & \left. + \tilde{f}_1 \frac{N_0}{t} \left[k_0 + \left(\frac{n a}{m b} \right)^2 (1 - k_0) \right] - 2 c_0 E_1 \tilde{f}_1^3 (\alpha_{k1} + \alpha_{k2}) \left(\frac{n\pi}{b} \right)^2 \right\} \end{aligned} \quad (37)$$

where $\tilde{f}_1 = f_1/t$ is the dimensionless displacement, N_0 is the total load, k_0 is parameter of the load ($0 \leq k_0 \leq 1$) defining uniform compressive forces: $N_x = k_0 N_0$ and $N_y = (1 - k_0) N_0$.

The above equation gives the dimensionless dynamic lateral displacements versus the time. Dimensionless displacement $f_1(\tau)$ is numerically solved.

A critical load of the static problem can be written as

$$\left(\frac{N_0}{t} \right)_{CR} = \min_{m,n} \frac{1}{k_0 + \left(\frac{n a}{m b} \right)^2 (1 - k_0)} \left[\frac{E_1 t^2}{(1-\nu^2)} (c_1 - c_2 \alpha_{\Phi_1} - c_3 \alpha_{\Phi_2}) \left(\frac{m\pi}{a} \right)^2 \left[1 + \left(\frac{n a}{m b} \right)^2 \right]^2 \right] \quad (38)$$

Finally, the equation of dynamic equilibrium of the plate has a form:

$$\frac{\partial^2 \tilde{f}_1}{\partial \tau^2} = \frac{m^2 \pi^2}{a^2 c_{11} \rho_1} \left\{ \left[\frac{N_0(\tau)}{t} - \left(\frac{N_0}{t} \right)_{CR} \right] \left[k_0 + \left(\frac{n a}{m b} \right)^2 (1 - k_0) \right] \tilde{f}_1 - 2 c_0 E_1 t^2 (\alpha_{k1} + \alpha_{k2}) \tilde{f}_1^3 \right\} \quad (39)$$

The dynamic stability problem is analysed for a family of rectangular plates with simply supported edges and following dimensions: $t = 0.002$ m, $a = 0.16$ m, $b = 0.32$ m. Material constants of the plate: Young's modulus, $E_1 = 7.06 \cdot 10^4$ MPa, Poisson ratio $\nu = 0.33$, mass density $\rho_1 = 2800$ kg/m³ and the coefficient of the porosity $e_0 = 0.9$.

Numerical calculations an approach with the Runge-Kutta method were carried out. A linear relations between total load N_0 and load rate c [MPa/s] is assumed

$$\frac{N_0(\tau)}{t} = c \cdot \tau \quad (40)$$

Dimensionless parameter of the time is introduced as quotient of current values of load and upper critical load of the static problem

$$\tilde{\tau} = \frac{\tau}{\tau_{CR}} = \frac{N_0(\tau)}{N_{0,CR}} \quad (41)$$

where τ_{CR} – “critical” time when the load equals value for static buckling problem.

The condition of allowable stress is performed as $\sigma_{eq,max} \leq \sigma_{all} = 240$ MPa, where $\sigma_{eq,max}$ is the maximal equivalent stress and σ_{all} is allowable stress. Biaxial loading is described by loading state: $N_y = (1 - k_0)N_0$, $N_x = k_0N_0$. In general the numerical results are obtained using selected values of load velocity “ c ” and values of load parameter k_0 . The results of numerical calculations in the form of family curves are presented in Fig. 4 ($k_0 = 0.33$) and Fig. 5 ($k_0 = 0.75$). It was noticed that dynamic resistance increase with the increase of the velocity of load. Simultaneously, we can indicate that is clearly change of shape of buckling. Dashed lines mark curves correspond to the static shape of buckling and continuous lines are the dynamic shape of buckling. If the numbers of half-waves increase then maximum deflection decreases with the increase of load velocity. In this paper the Volmir criterion for dynamic loads is assumed. According to this criterion the critical load defined the time, in which the deflection of a plate equals the value of the thickness of a plate ($\tilde{f}_1 = 1$).

5. FEM analysis of dynamic stability of the rectangular plate

A numerical analysis of an isotropic plate made of a porous material was carried out by Magnucki *et al.* (2006). Bending and elastic buckling obtained analytically and numerically (FEM) were presented by them.

For better assessment of the previous numerical results, additional FEM studies of the effect of ratio load k_0 on the dynamic response of metal foam rectangular plate has been carried out with ANSYS 5.7. A discrete model of the plate was built from finite elements SHELL181 and it is a four-nodes element with six degrees of freedom at each node: translations in the x , y , and z directions, and rotations about

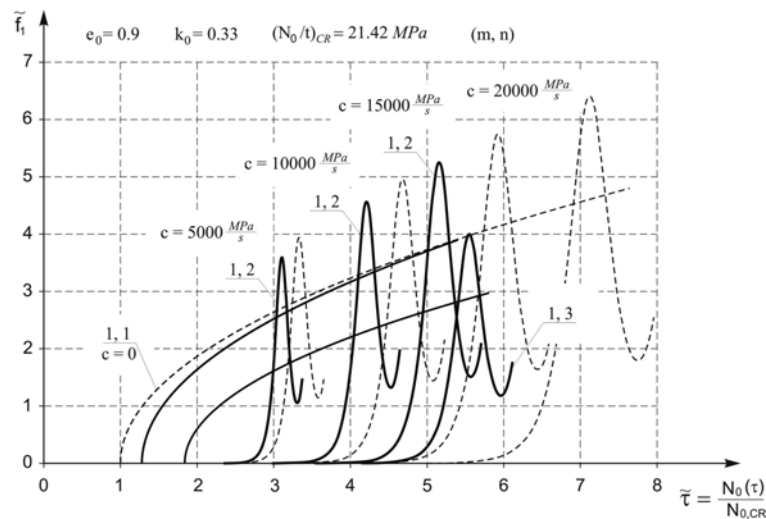


Fig. 4 The deflection of a plate versus parameter $\tilde{\tau}$ with dominant load N_y ($k_0 = 0.33$)

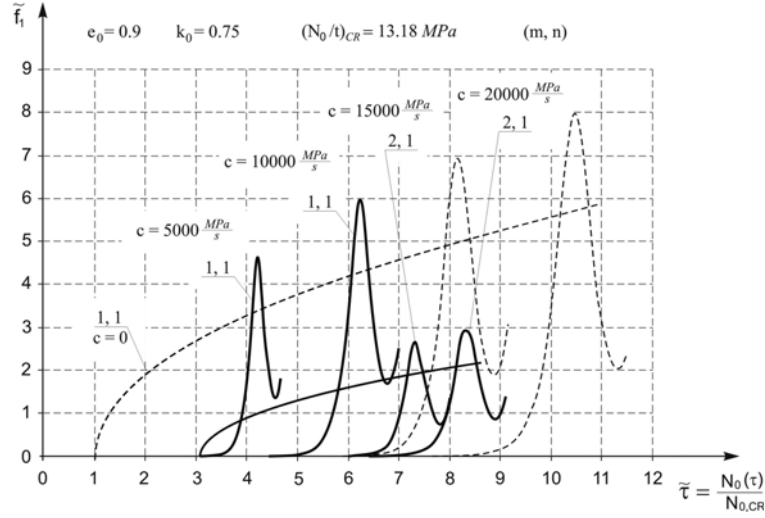


Fig. 5 The deflection of a plate versus parameter $\tilde{\tau}$ with dominant load N_x ($k_0 = 0.75$)

the x , y , and z -axes (Elements reference, ANSYS 5.4, Ansys Inc., 1994). This element was associated with isotropic, linear elastic material properties. Large Displacement Transient option with large deflections was selected. Basing on Eqs. (1) and (2) mechanical and physical properties of SHELL181 element can calculate after integrating on the interval $1/2 \leq \zeta \leq 1/2$

$$E = E_1 c_{24} = E_1 \left(1 - \frac{2e_0}{\pi} \right) \quad (42)$$

$$\rho = \rho_1 c_{11} = \rho_1 \left(1 - \frac{2e_m}{\pi} \right) \quad (43)$$

A full model of rectangular plate consisting a metal foam could also be generate using standard layered shell element (SHELL99). The element has six degrees of freedom at each node. Preliminary research of dynamic stability of a plate showed that in this case the material properties varying through thickness of the cross-section of FEM model should be discretized with number of layers (NL) of constant properties grater then $NL = 27$. Young modulus (E) in the mid-plane of each layer were calculated from Eq. (1). Maximum difference of displacement values calculated using SHELL181 and SHELL99 elements is not greater then 2% (for $NL = 27$). If $NL > 27$ then difference of displacement values decreases but time of solution violently increases.

Three cases of load were selected: $k_0 = 0.25$, $k_0 = 0.50$ and $k_0 = 0.75$. The geometrical characteristics of the plate were as follows: $t = 0.002$ m, $a = 0.16$ m, $b = 0.32$ m. For the FEM simulation, following mechanical and physical constants are chosen: $E_1 = 7.06 \cdot 10^4$ MPa, $\nu = 0.33$, $\rho_1 = 2800$ kg/m³, $e_0 = 0.9$, and the load rate $c = 20$ GPa/s.

The transient dynamic analysis using the full method was selected and the automatic time increment (load-step) of the integration was based on the response of the structure (Structural Analysis Guide, ANSYS 5.4, Ansys Inc., 1994). Let consider the case when $k_0 = 0.25$. Fig. 6 shows the analytical-

numerical (A-N) and FEM results of the dynamic problem. The curves show the deflection time-history for a dynamical stability of a metal foam plate. The displacement perpendicular to the surface of a plate rapidly increase and achieves the maximum value. Elastic deformation of the plate after $\tau = 6.8$ ms is shown in Fig. 7. There is practically no difference between the curves for analytical-numerical (A-N) and FEM solutions. Maximum dynamic displacement of the plate is after $\tau = 5.1$ ms. In the case of the numerical solution (Eq. 39) the time is $\tau = 5.4$ ms. The difference of time of the dynamic response for both methods equals 5.5%.

The result of dynamic displacement for the plate for $k_0 = 0.50$ is shown in Fig. 8. The dynamic response of the plate is presented in Fig. 9. In this case, the difference of time for A-N ($\tau = 5.8$ ms) and FEM ($\tau = 5.6$ ms) is equal 3.5%. Fig. 10 shows an example of dynamic displacement of a plate for $k_0 = 0.75$. The dynamic response of the plate after $\tau = 5.1$ ms is presented in Fig. 11. The difference of the time for A-N and FEM solution does not exceeds 7%. In all presented cases, the dynamic

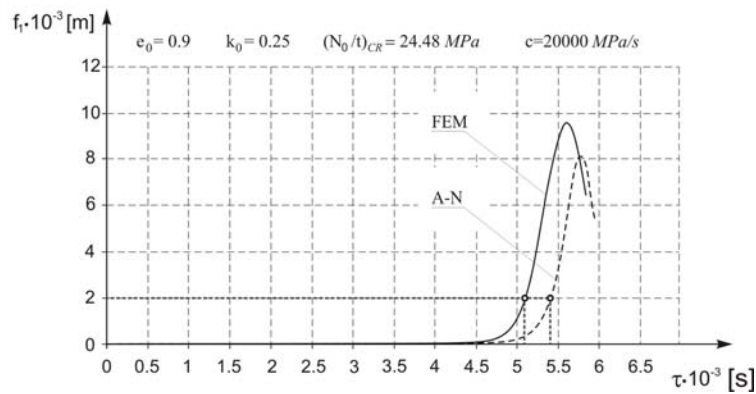


Fig. 6 Dynamic displacement versus time ($k_0 = 0.25$)

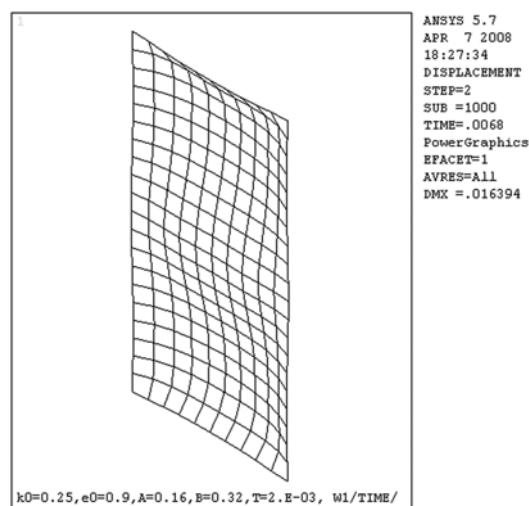


Fig. 7 Dynamic response of a plate after time $\tau = 6.8$ ms ($k_0 = 0.25$)

displacements of plates rapidly increase, when the dynamic load exceeds value of critical load of static buckling problem ($N_{0,CR}$).

The influence of coefficient of porosity on the dynamic stability of a plate has been also analysed. The analysis was carried out for porous rectangular plates with the following parameters: $a = 0.16$ m, $b = 0.36, 0.40$ m, $t = 0.002$ m, $e_0 = 0.9, 0.99$, $k_0 = 0.25$, $E_1 = 7.06 \cdot 10^4$ MPa, $\nu = 0.33$, $\rho_1 = 2800$ kg/m³, $c = 20$ GPa / s.

The comparison of results between A-N and FEM solutions are presented in Figs. 12-13. Dashed curved lines mark curves correspond to the A-N solutions and continuous curved lines are the FEM solutions. The parameter of the porosity is presented by suitable symbols on the curves. Figs. 12-13 present the deflection time-history for a dynamical stability of a plate carried out to two selected examples. The first example (Fig. 12) represents the dynamic response of a rectangular plate with the

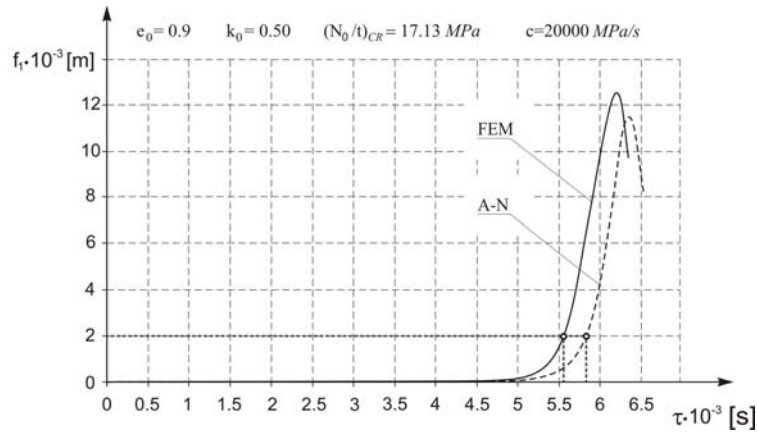


Fig. 8 Dynamic displacement versus time ($k_0 = 0.50$)

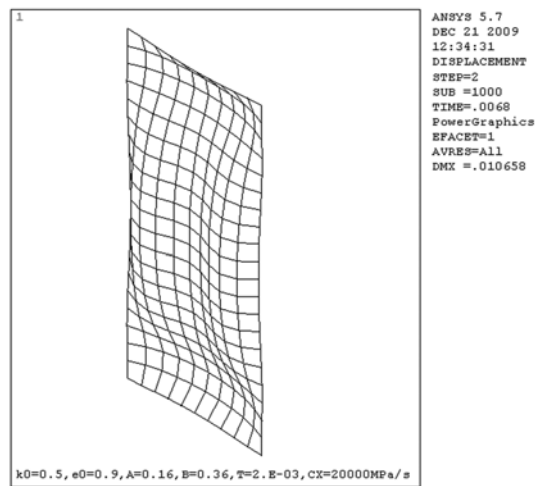
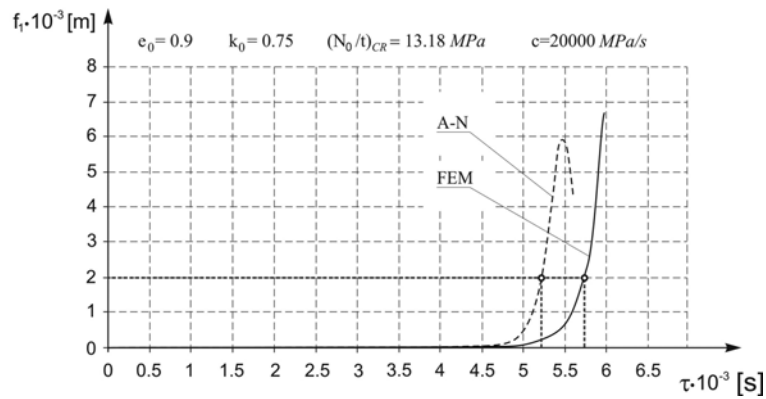
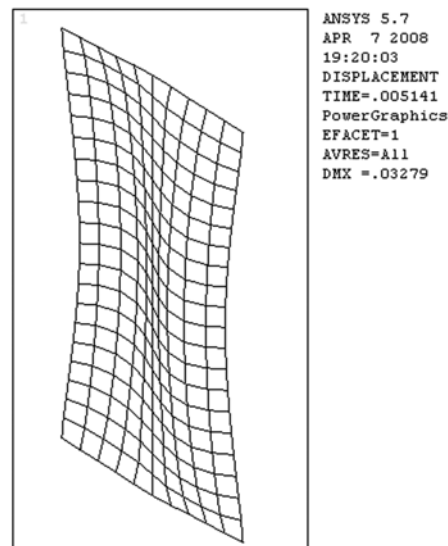


Fig. 9 Dynamic response of a plate after time $\tau = 6.8$ ms ($k_0 = 0.50$)

Fig. 10 Dynamic displacement versus time ($k_0 = 0.75$)Fig. 11 Dynamic response of a plate after time $\tau = 5.1$ ms ($k_0 = 0.75$)

length $b = 0.40$ m. When $e_0 = 0.9, 0.99$ the “critical” value of the time (Volmir criterion) is 5.44 ms, 5.07 ms (A-N), respectively. Results of FEM analysis are 5.25 ms, 4.70 ms, respectively and are lesser approximately to 7% then in the case of A-N analysis.

Fig. 13 compares the results obtained for $b = 0.36$ m. In this case and A-N analysis, time in which the displacement of a plate equals value arising from Volmir criterion are 5.47 ms ($e_0 = 0.9$) and 5.04 ms ($e_0 = 0.99$).

The results obtained show that considering the porosity characteristic of metal foam material leads to a increase in start time of dynamical response.

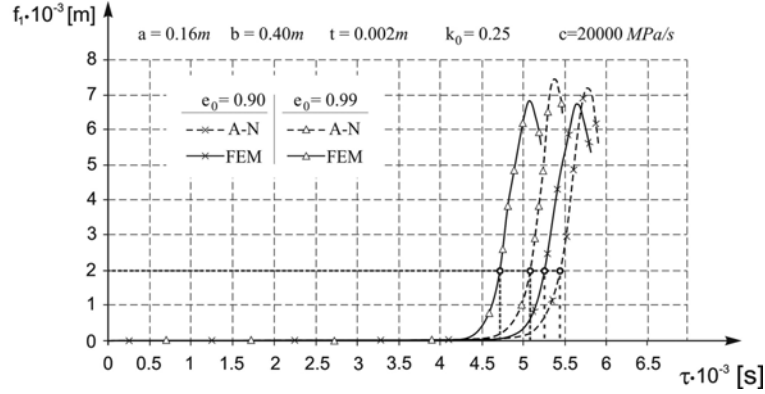


Fig. 12 Dynamic displacement versus time for various values of coefficient of the porosity ($b = 0.40 m$)

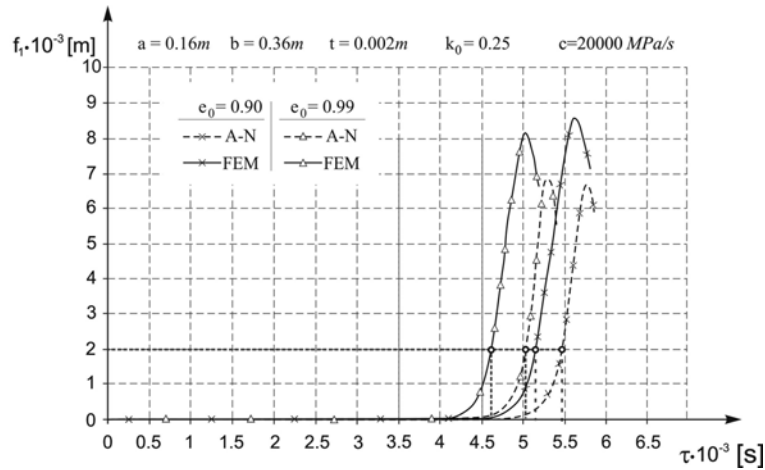


Fig. 13 Dependence of the deflection on time for various values of coefficient of the porosity ($b = 0.36m$)

6. Conclusions

The paper presents the problem of the dynamic stability of metal foam rectangular plates. The non-linear hypothesis of deformation of plane cross section of the plate was positively numerically verified by FEM. The transverse shear effect was taken into account. The dynamic resistance of the plate increases with a decrease of rate load. The general solution to the seven differential equations of dynamic stability enables one equation of dynamic equilibrium of the plate. Computed results show that dynamic behaviour of a metal foam plate depends on the coefficient of porosity e_0 , load rate c and parameter of load k_0 . Discrete model of a metal foam plate has been consisted from 27 layers. For bigger values of e_0 bigger numbers of layers through out thickness of a plate should be taken into account. In this case, difference between A-N and FEM results become smaller.

The present study is an introduction to a series of papers devoted to dynamic stability of metal foam rectangular plates.

References

- Abramovich, H. and Grunwald, A. (1995), "Stability of axially impacted composite plates", *Compos. Struct.*, **32**, 151-158.
- Ashby, M.F., Evans, A.G., Fleck, N.A., Gibson, L.J., Hutchinson, J.W. and Wadley, H.N.G. (2000), *Metal foams: a design guide*, Butterworth-Heinemann, Boston.
- Bakker, M.C.M., Rosmanit, M., Hofmeyer, H. (2007), "Elastic post-buckling analysis of compressed plates using a two-strip model", *Thin Wall. Struct.*, **45**, 502-516.
- Banhart, J. (2001), "Manufacture, characterization and application of cellular metals and metal foams", *Prog. Mater. Sci.*, **46**, 559-632.
- Bart-Smith, H., Hutchinson, J.W. and Evans, A.G. (2001), "Measurement and analysis of the structural performance of cellular metal sandwich construction", *Int. J. Mech. Sci.*, **43**, 1945-1963.
- Carrera, E. (2000), "An assessment of mixed and classical theories on global and local response of multilayered orthotropic plates", *Compos. Struct.*, **50**, 183-198.
- Carrera, E. (2001), "Developments, ideas, and evaluations based upon Reissner's mixed variational theorem in the modeling of multilayered plates and shells", *Appl. Mech. Rev.*, **54**, 301-329.
- Carrera, E. (2003), "Historical review of Zig-Zag theories for multilayered plates and shells", *Appl. Mech. Rev.*, **56**, 287-308.
- Carrera, E., Brischetto, S. and Robaldo, A. (2008), "Variable kinematic model for the analysis of functionally graded material plate", *AIAA Journal.*, **46**(1), 194-203.
- Choi, J.B. and Lakes, R.S. (1995), "Analysis of elastic modulus of conventional foams and of re-entrant foam materials with a negative Poisson's ratio", *Int. J. Mech. Sci.*, **37**(1), 51-59.
- Debowski, D. and Magnucki, K. (2006), "Dynamic stability of a porous rectangular plate", *PAMM*, **6**(SPI), 215-216.
- Elements Reference*, ANSYS 5.4, Ansys Inc., 1994.
- Eshmatov, B.K. (2007), "Nonlinear vibrations and dynamic stability of viscoelastic orthotropic rectangular plates", *J. Sound. Vib.*, **300**, 709-726.
- Evans, A.G., Hutchinson, J.W. and Ashby M.F. (1999), "Multifunctionality of cellular metal system", *Prog. Mater. Sci.*, **43**, 171-221.
- Fares, M.E. and Elmarghany, M.K. (2008), "A refined zig-zag nonlinear first order shear deformation theory of composite laminated plates", *Compos. Struct.*, **82**, 71-83.
- Kovacik, J. (1999), "Correlation between Young's modulus and porosity in porous materials", *J. Mater. Sci. Lett.*, **18**, 1007-1010.
- Kovacik, J. (2001), "Correlation between shear modulus and porosity in porous materials", *J. Mater. Sci. Lett.*, **20**, 1953-1955.
- Magnucki, K. and Stasiewicz, P. (2004a), "Elastic bending of an isotropic porous beam", *Int. J. Appl. Mech. Eng.*, **9**(2), 351-360.
- Magnucki, K. and Stasiewicz, P. (2004b), "Elastic buckling of a porous beam", *J. Theor. Appl. Mech.*, **42**(4), 859-868.
- Malinowski, M. and Magnucki, K. (2005), "Deflection of an isotropic porous cylindrical panel", *Proceeding of the 8th SSTA conference*, Eds. Pietraszkiewicz, W. and Szymczak, C. Taylor & Francis ; London, New York, Philadelphia, Singapore., 143-147.
- Magnucki, K., Malinowski, M., Kasprzak, J. (2006), "Bending and buckling of rectangular porous plate", *Steel. Compos. Struct.*, **6**(4), 319-333.
- Mielniczuk, J. and Malinowski, M. (2005), "Models of porous materials for design of construction shell elements", *Pojazdy Szybowe*, **3**, 15-21, (in Polish).
- Mielniczuk, J., Malinowski, M., Kuligowski, P. (2006), "Porous shell elements for wagon roof of railway vehicles", *Pojazdy Szybowe*, **2**, 1-5, (in Polish).
- Qatu, M.S. (2004), *Vibration of laminated shells and plates*, Elsevier, Amsterdam.
- Ramamurty, U. and Paul, A. (2004), "Variability in mechanical properties of metal foam", *Acta Mater.*, **52**, 869-876.
- Reddy, J.N. (2000), "Analysis of functionally graded plates", *Int. J. Numer. Meth. Eng.*, **47**, 663-684.

- Sahu, S.K. and Datta, P.K. (2007), "Research advances in the dynamic stability behavior of plates and shells: 1987-2005 - Part 1: Conservative systems", *Applied Mechanics Reviews*, **60**, 65-75.
- Structural Analysis Guide*, ANSYS 5.4, Ansys Inc., 1994.
- Szcześniak, W. (2000), *Selected problems of dynamic of plates*, Oficyna Wydawnicza Politechniki Warszawskiej, Warszawa (in Polish).
- Wang, C.M., Reddy, J.N., Lee, K.H. (2000), *Shear deformable beams and plates*, S. Elsevier Sciences., Amsterdam, Lausanne, New York, Oxford, Singapore, Tokyo.
- Yang, J., Liew, K.M., and Kitipornchai, S. (2006), "Imperfection sensitivity of the post-buckling behavior of higher-order deformable graded plates", *Int. J. Solids. Struct.*, **43**, 5247-5266.
- Zhang, T., Liu, T. and Luo, J. (2004), "Nonlinear dynamic buckling of stiffened plates under in-plane impact load", *J. Zhejiang University Science*, **5**(5), 609-617.